CERN–PPE/95-116
24 July 1995

Search for Direct Photons from S-Au Collisions at 200 GeV/u

R. Baur[2], A. Breskin[3], R. Chechik[3], A. Drees[2], C. Jacob[1], U. Faschingbauer[1], P. Fischer[2], Z. Fraenkel[3], E. Gatti[4], P. Glässel[2], Th. Günzel[2], C. P. de los Heros[3], F. Hess[1], D. Irmscher[2,*], B. Lenkeit[2], L. H. Olsen[2], Y. Panebrattsev[1,c], A. Pfeiffer[2], I. Ravinovich[3], P. Rehak[5], A. Schön[2], J. Schukraft[6], M. Sampietro[4], A. Shor[3], H. J. Specht[2], V. Steiner[3], S. Tapprogge[2], G. Tel-Zur[3], I. Tserruya[3], Th. Ullrich[2], J. P. Wurm[1]

(CERES Collaboration)

Abstract

The CERES experiment has measured inclusive photon production in S-Au collisions of 200 GeV/nucleon at the CERN SPS. No evidence for direct emission of photons was found. For the kinematic region $2.1 < y < 2.65$ and 0.4 GeV/c $< p_\perp <$ 2.0 GeV/c the yield and $p_\perp$-dependence of the observed photons are well reproduced by hadron decays. Furthermore, their production rate is found to be proportional to the charged particle density. The significance of the results is limited by systematic errors, which set an upper limit of 7% for any unconventional photon source in central S-Au collisions.

(submitted to Zeitschrift für Physik C)

*) Doctoral Thesis of D. Irmscher, Universität Heidelberg (1993)
1) Max-Planck-Institut für Kernphysik, 69117 Heidelberg, Germany
2) Physikalisches Institut der Universität Heidelberg, 69120 Heidelberg, Germany
3) Weizmann Institute, Rehovot 76100, Israel
4) Politecnico di Milano, 20133 Milano, Italy
5) Brookhaven National Laboratory, Upton, NY 11973, USA
6) CERN, 1211 Geneva 23, Switzerland
c) visiting from JINR, Dubna, Russia

1 Introduction

Direct photons are commonly accepted as a promising probe for the elusive quark gluon plasma, since they do not interact strongly and thus carry information about the hot early stage of the interaction. The difficulty in their measurement in heavy-ion collisions is the huge background due to hadron decays, mainly π° and η. The production rate of direct photons from quark-antiquark annihilation, quark-gluon-Compton and hadron-hadron scattering in a hot and dense hadronic system has been investigated theoretically by several authors [1, 2]. Even though the absolute values of the predicted yields vary by a factor of up to 5, some properties seem to be rather well established at SPS beam energies. Direct photons from partonic and hadronic processes are similar in rate. Their overall yield is of the order of, or smaller than 10% of the inclusive photon production, and even their $p_\perp$-distribution is not very different from that of the hadron decay photons. However, the production of direct photons is expected to scale with the square of the charged particle density dN_{ch}/dy if volume effects are taken into account. In contrast, the number of photons from hadron decays is obviously proportional to dN_{ch}/dy. Presently, experiments [3, 4] are barely accurate enough to detect the highest predicted absolute yields, but the quadratic multiplicity dependence may provide a more sensitive tool to disentangle direct photons from the hadron decay contribution.

Here we present the measurement of inclusive photon production in S-Au collisions at 200 GeV/nucleon performed by the CERES/NA45 experiment.

2 Experimental setup

CERES (Fig. 1) is an experiment dedicated to the measurement of e^+e^--pair production in pp-, pA- and AA-collisions at central rapidity ($2.1 < \eta < 2.65$) in the mass range up to $m_{ee} < 2000$ MeV/c^2. A detailed description of the CERES experiment can be found in refs. [5, 6]. Here we summarize the most relevant features of the detector. Particle identification and tracking are based on two azimuthally symmetric RICH (Ring Imaging CHerenkov) detectors operated with a Cherenkov threshold ($\gamma_{thr} \approx 32$) high enough to suppress signals from the large number of hadrons produced in the collisions to a very low level. Momentum and charge information are provided by a superconducting double solenoid between the RICH detectors, which locally deflects the particles in azimuthal (ϕ) direction according to $\Delta\phi = 0.12$ rad/p (GeV/c), but leaves the polar angle θ unchanged. The magnetic field (indicated in Fig. 1) is shaped such that the region of RICH-1 is free of field, while in RICH-2 the field lines point back to the target. This field shaping guarantees straight particle trajectories inside the radiators which lead to clear ring images and preserves the original particle direction and the e^+e^--pair opening angle in RICH-1. In both detectors the Cherenkov photons are focused by a spherical mirror onto a plane upstream of the target, which allows their detection in UV-sensitive photon detectors outside the huge flux of forward going particles [7]. A silicon pad detector (SiPD) [8] close to the target supplies charged particle multiplicity N_{ch} both for first-level triggering and off-line analysis. In addition, a silicon drift chamber (SiDC) [9] supports the pattern recognition and also measures $dN_{ch}/d\eta$. In order to minimize the number of photon conversions and hence the combinatorial e^+e^--pair background, a segmented target of 40 gold disks each 50 μm thick with a diameter of 600 μm separated by 1.5 mm was used.

The capability of the CERES spectrometer to recognize and reject photon conversions, the dominant background for the e^+e^--pair measurement, opens the possibility to carefully study the production of photons using the conversion method with the target

(2.3% of a radiation length) acting as converter. The conversions are identified by a typical pattern in the RICH detectors. Since the opening angle of e^+e^--pairs originating from converted photons is a few mrad only, the pair is not or barely opened in RICH-1, while in RICH-2 electrons and positrons are deflected by the magnetic field in opposite azimuthal directions, keeping the polar angle θ unchanged. Hence a conversion has a V-shaped signature with an unresolved double ring in the first and two distinct rings in the second RICH. A example for such a V-pattern is shown in the blowup of an event display of RICH-1 and RICH-2 in Fig. 2.

Charged pions can also be reconstructed for momenta above 5.5 GeV/c where they exceed the Cherenkov threshold and radiate enough Cherenkov photons to produce a recognizable ring image. They can be distinguished easily from electrons up to $p \simeq 20$ GeV/c by the smaller ring radius, which also provides an independent measurement of the pion momentum.

3 Data analysis

In the CERES experiment, the event reconstruction relies entirely on the RICH detectors. Cherenkov rings are reconstructed without an *a priori* knowledge of the ring centers. In the first step, the event is cleaned from obvious background signals originating from electronic noise and physics sources like highly ionizing particles, which unnecessarily complicate the ring recognition. The remaining event is searched for ring candidates using a point-to-ring Hough transformation. In the vicinity of these candidates, single photon hits are reconstructed, and a ring of asymptotic radius is fitted to these hits. In order to cope with the large number of background hits in the environment, each hit is weighted by a Gaussian potential according to its distance from the ring. Finally, true Cherenkov rings are filtered from random combinations of hits accidentally combined to 'fake' rings employing an artificial neural network. The neural network operates on numerous variables describing the rings and their environment. It is significantly more efficient in rejecting fake rings than any standard analysis technique based on quality cuts on the same variables. For pions the ring reconstruction is essentially the same, except that the ring radius is no longer known. However, it is constrained to be equal in RICH-1 and RICH-2 and consistent with the ϕ-deflection angle.

Rings in both RICH detectors are combined to tracks, identified by their common θ-angle. In order to reduce ambiguities in the track reconstruction, only tracks with a ϕ-deflection corresponding to $p_\perp > 50$ MeV/c are accepted. Conversion candidates are defined as V-shaped pairs of tracks with a common ring in the first RICH and a minimum opening angle of $\Delta\phi > 3$ mrad in the second RICH. A total of $8.5 \cdot 10^5$ S-Au collisions selected by two different multiplicity (centrality) triggers have been analyzed. In this sample 95,000 conversions and 77,000 pions were reconstructed.

In order to evaluate the photon $p_\perp$-spectrum, a correction for the reconstruction efficiency within the acceptance and the smearing of the $p_\perp$-spectrum due to the momentum resolution is needed. This correction function is obtained by generating photons with a given $p_\perp$-spectrum and tracking them through a GEANT Monte-Carlo simulation [10] of the CERES detector. Measured detector parameters, like the primary number of Cherenkov photons, the width of the Cherenkov hits, their spread around the nominal ring radius and local gain variations, are fed into this simulation. The digitized Monte-Carlo event is overlaid with data to simulate realistic background conditions. This mixture is then passed through the analysis chain. The ratio of the generated to the reconstructed

Monte-Carlo $p_\perp$-spectra, shown in Fig. 3, is used to correct the measured photon $p_\perp$-spectrum. In the $p_\perp$-region 0.4 to 1.5 GeV/c the correction function decreases only slowly with an average reconstruction efficiency of $\sim$ 20%. For lower $p_\perp$, photon conversions are lost due to the single track $p_\perp$-cut of 50 MeV/c and the correction becomes large. Above 1.5 GeV/c the correction function decreases more rapidly, as – due to the limited momentum resolution – more and more photons are reconstructed at too large $p_\perp$.

The measured photon $p_\perp$-spectrum is contaminated by e^+e^--pairs from π^o Dalitz decays, which – due to their low mass and resulting small opening angle – are undistinguishable from photon conversions in the RICH detectors. The necessary correction was calculated with a Monte-Carlo method similar to the one described above. Because of the limited double ring resolution of $\sim$ 8 mrad, about 50% of all π^o Dalitz decays produce a conversion-like pattern in the RICH detectors. Including the opening angle dependence of the reconstruction efficiency of e^+e^--pairs, this results in an 18% contamination of the inclusive photon spectrum. The contribution of π^o Dalitz decays is nearly independent of $p_\perp$. It is subtracted from the measured photon spectrum.

For pions the efficiency correction is much more sensitive to the precise knowledge of detector parameters than it is for photon conversions. A normalization of the photon yield to the measured number of charged pions therefore leads to unacceptable systematic errors. Instead, the yield is normalized to the charged particle density $dN_{ch}/d\eta$ at $\eta = 2.4$, which is determined from the amount of energy deposited in the silicon pad detector ($1.7 < \eta < 3.7$). Each of the 64 pads is analyzed as a convolution of Landau distributions. The multiplicity sum of all pads (N_{ch}) is corrected for inactive areas of the detector and the small contribution from photon conversions as well as from δ-electrons produced in the target. In an asymmetric collision system like S-Au the center-of-mass rapidity y_{cm} and therefore the maximum charged particle density shifts towards target rapidity with decreasing impact parameter. Consequently $dN_{ch}/d\eta$ at $\eta = 2.4$, the relevant quantity for our photon measurement, is not strictly proportional to N_{ch} measured in $1.7 < \eta < 3.7$. The uncertainty of the vertex position in the segmented target prevents us from extracting the non-linearity from the silicon pad data itself. We have used data from S-W [11] and S-Au [12] collisions obtained at the same beam energy to quantify the non-linearity. It amounts to approximately 10% over the N_{ch}-range covered by our measurement. The fully corrected multiplicity distribution is shown in Fig. 4. The average multiplicity of our data sample is $< dN_{ch}/d\eta > = 135$ at $\eta = 2.4$. Note that the average includes data taken with two different multiplicity thresholds. Nevertheless, the sample is dominated by central collisions and in the following we refer to it as central S-Au collisions.

4 Comparison of the photon $p_\perp$-spectrum with known hadronic sources

Fig. 5 shows the inclusive photon $p_\perp$-spectrum for S-Au collisions at 200 GeV/u measured in the rapidity range $2.1 < y < 2.65$. The expected contribution of all known hadron decays to the inclusive spectrum is also shown. The expected photon yield is calculated using a Monte-Carlo method. It assumes that within our rapidity acceptance the invariant cross section $d^3\sigma/dp_\perp^2\,dy$ factorizes in $p_\perp$ and y, such that the distributions can be treated separately. The $dN_{ch}/d\eta$ distribution for pions follows a fit to measured data [12]. The π^o $p_\perp$-spectrum is generated starting with a distribution measured for negative particles under similar conditions [13]. This spectrum is modified iteratively such that the resulting pion $p_\perp$-spectra, including pions from the decay of higher mass particles, describes measured $p_\perp$-spectra from various heavy-ion experiments [13, 14, 15, 16] in different kinematical regions. Photons from decays of heavier mesons like η, η' and ω are included employing known production cross sections [17] and branching ratios [18], assuming $m_\perp$-scaling [19] and modifying the width of their rapidity distribution to reflect the ratio of $\sigma_{central}/\sigma_{total}$ measured in p-p collisions [17]. It is important to note that, due to the iterative procedure, the resulting photon $p_\perp$-spectrum is rather insensitive to the exact choice of the initial $p_\perp$- and y-distribution.

In order to compare to data, the generator result must be normalized to the measured average charged particle density. Because no accurate data for $(d\sigma_{\pi^o}/d\eta)/(d\sigma_{N_{ch}}/d\eta)$ is available for S-interactions with heavy targets, a starting value of 0.46 measured in p-p collisions [17] at $y_{cm} = 0$ is used. We assume that at $y_{cm} = 0$ the composition of produced particles will not change going from p-p to S-Au collisions, which is supported by the similarity in particle composition found for S-Ag [14] and p-p [17] data at $y_{cm} = 0$. However, due to the higher degree of stopping in nuclear collisions, more charged baryons are shifted into the pseudorapidity region $2.1 < \eta < 2.65$. An extrapolation of the baryon density measured in S-Ag (at $y < 3$) and S-Au (at $y > 3$) reactions [14] is used to correct $(d\sigma_{\pi^o}/d\eta)/(d\sigma_{N_{ch}}/d\eta)$, reducing its value to 0.44.

The shape as well as the absolute yield of the $p_\perp$-distribution are well described by the known hadronic sources, clearly visible in Fig. 5. For a quantitative comparison, both $p_\perp$-spectra are integrated in the range $0.4 < p_\perp < 2.0$ GeV/c, resulting in a ratio r_γ of photons per charged particle:

$$r_\gamma = \left(\frac{dN_{ch}}{d\eta}\right)^{-1} \int \frac{dN_\gamma}{dp_\perp} dp_\perp \qquad (1)$$

Integrated over the full phase space, r_γ is $\sim$ 1 for photons from hadron decays. For $2.1 < y < 2.65$ and $0.4 < p_\perp < 2.0$ GeV/c the value is reduced to 0.09. In the same region we measure for the inclusive photon yield 0.091 ± 0.0004, quoting only statistical errors. The accuracy of the result is limited by the much larger systematic errors. The individual contributions are discussed below, quantified in terms of r_γ. The errors reflect the uncertainty of the photon yield at low $p_\perp$, for large $p_\perp$ the errors increase significantly. For those errors with a bell-shaped error distribution function the *rms* is quoted (for asymmetric cases, the *rms* for the positive and negative part of the distribution are given separately), otherwise upper and lower limits of a uniform distribution are given.

Systematic errors in the measurement:

• The photon reconstruction efficiency depends on detector parameters which are known only with limited accuracy. The most critical parameters, namely the number of Cherenkov photons per ring, the spread of photon hits around the nominal radius and the width of the detector response to a single Cherenkov photon were varied within these limits. The combined uncertainty is $\sigma \approx +2.7\%, -5\%$. The efficiency correction is not sensitive to the exact shape of the input $p_\perp$-distribution. Different fits to parameterize the correction function contribute less than 2% to the systematic error.
• The subtraction of the π^o Dalitz decay contamination depends on the correct description of the opening angle distributions of both Dalitz decays and photon conversions. Monte-Carlo studies show a variation of the photon yield due to these uncertainties of $\pm$ 5%.
• The conversion method relies on the exact knowledge of the converter thickness. Besides the target, all other materials in the target area, like the silicon detectors, radiator windows etc. contribute to the conversion probability. All these materials were carefully included in a GEANT Monte-Carlo simulation of the target area. Following reference [10], the

conversion probability is accurate to $\pm$ 2.5%. Including an additional statistical error of $\pm$ 1.5%, due to the limited amount of Monte-Carlo events available for this evaluation, the overall error is $\sigma = 3\%$.

• The charged particle density $dN_{ch}/d\eta$ is known within $\pm$ 5%. The determination of N_{ch} with the silicon drift detector gives a result consistent with that obtained from the silicon pad detector. Due to imperfections of the drift detector available in 1992, the accuracy could, however, not be increased. The systematic error of the average charged particle density caused by extrapolating N_{ch} from the rapidity acceptance of the silicon pad counter to $dN_{ch}/d\eta$ in the RICH acceptance is negligible ($< 1\%$).

Systematic errors in the photon yield from hadron decays:

• The expected photon yield varies due to uncertainties of the input $p_\perp$- and y-distributions for the generator. Different slopes of the pion $p_\perp$-distribution change the final yield in the range +3.5%,−5.3%. The width of the rapidity distribution has been varied by 30%. The error on r_γ is +2.4%, −3.9%.

• The contribution from heavier mesons to the photon yield is dominated by the η-meson. In the hadron decay generator the total cross sections for the η-meson production was fixed to 0.1 relative to the π°. Comparing all available data [15, 17, 20], η/π° seems to be reliably known to within $\pm$ 30%. In particular, there is significant evidence that in S-Au η/π° remains unchanged compared to p-p collisions [15]. The resulting systematic error is estimated to be $\pm$ 2.4%.

• For the normalization, a value of $n_{\pi^\circ}/N_{ch} = 0.44$ was used. The statistical and systematical errors of the measurement [17] as well as the uncertainty in the estimation of the the different amounts of charged baryons shifted into the rapidity region $2.1 < \eta < 2.65$ in p-p and S-Au collisions leads to an overall error of $\sigma = 5.4$ %.

In order to deduce the overall systematic error of r_γ, the different error distribution functions are convoluted. The FWHM of the resulting distribution is then quoted as systematic error. For the measurement and the estimation of the hadron decays we find:

$$r_{data} = 0.091 \pm 0.0004\, stat. \; {}^{+0.004}_{-0.008}\, syst. \tag{2}$$

$$r_{hadr} = 0.090 \pm 0.006\, syst. \tag{3}$$

Within the errors both values are equal. The fraction of direct photons may be expressed as the surplus of the measured over the expected photon yield from hadron decays:

$$\frac{N_\gamma^{dir}}{N_\gamma^{hadr}} = \frac{r_{data}}{r_{hadr}} - 1 = 1 \; {}^{+8.5}_{-13}\% \tag{4}$$

The errors of this ratio set an upper limit of 10% at a 90% confidence level on any contribution of direct photons to the inclusive photon yield.

5 Multiplicity dependence of the photon production

The multiplicity dependence of the photon yield provides an additional tool to search for direct photons independent of the difficulties of the absolute normalization discussed above. While the photon yield from hadron decays must be proportional to the charged particle density, the rate of thermal photons is expected to scale with the square of the particle density at time of their creation, independent of the underlying production mechanism. Inevitably, the yield of photons normalized to some variable proportional to dN_{ch}/dy results in a constant value for photons from hadron decays, whereas a contribution of direct photons would be signaled by a rise with dN_{ch}/dy. Here we adopt two different strategies of normalization. In the first approach shown in Fig. 6a we normalize to $dN_{ch}/d\eta$ measured by the silicon pad detector, in other words, r_γ obtained in Section 4 is analyzed as a function of $dN_{ch}/d\eta$. Mandatory for such a study is an accurate correction of the non-linear multiplicity scale, as discussed in chapter 3. The second method avoids this problem by normalizing to the charged pions observed in the CERES spectrometer between $p_\perp = 1.3$ to 2.5 GeV/c. The multiplicity dependence of the ratio n_γ/n_π is plotted in Fig. 6b. The large uncertainty in the pion reconstruction efficiency, which previously prevented the use of pions for precise normalization of the photon yield, is irrelevant here since it mostly affects the absolute value of n_γ/n_π, but not its multiplicity dependence.

Both methods of normalization give the same result: The photon yield is proportional to the charged particle density. We find no evidence for a source of photons with a quadratic multiplicity dependence. In order to quantify the measurements we parameterize the normalized photon yield G assuming a contribution quadratic in $dN_{ch}/d\eta$:

$$G(dN_{ch}/d\eta) = C \cdot (1 + \alpha \cdot dN_{ch}/d\eta) \tag{5}$$

with $\alpha \cdot dN_{ch}/d\eta = N_\gamma^{direct}/N_\gamma^{hadron}$, i.e. the ratio of direct photons to photons from hadron decays, and the constant C which measures r_{hadr} (cf. Section 4) for Fig. 6a and, after correcting for the different $p_\perp$-acceptance of photons and pions, N_γ^{hadron}/N_π for Fig. 6b. The fits are also shown on the figures, the numerical values of the slope parameters are:

$$\alpha = (+0.5 \pm 1.4\, stat. \ {}^{+4.5}_{-1.5}\, syst.) \cdot 10^{-4} \tag{6}$$

$$\alpha = (-0.4 \pm 1.9\, stat. \ {}^{+6}_{-4.5}\, syst.) \cdot 10^{-4} \tag{7}$$

for Fig. 6a and b, respectively. Both values of α are consistent with zero within the statistical errors. The relevant sources of systematic errors on α are listed in the following.

Systematic errors normalizing to $dN_{ch}/d\eta$:

• As mentioned above, the main uncertainty is caused by the non-linearity between N_{ch} $(1.7 < \eta < 3.7)$ and $dN_{ch}/d\eta$ at $\eta = 2.4$. If no correction is applied r_γ rises trivially with N_{ch}, resulting in a false value of $\alpha = 8.5 \cdot 10^{-4}$. Obviously, the necessary correction is large. Comparing various methods to extract the correction we are confident that the uncertainty of α is not larger than ${}^{+4.5}_{-0.5} \cdot 10^{-4}$.
• There is a small but finite decrease of the photon reconstruction efficiency with $dN_{ch}/d\eta$. It was studied in detail by a Monte-Carlo simulation. In terms of α the error is slightly asymmetric: ${}^{+1.5}_{-3} \cdot 10^{-4}$.

Systematic errors on n_γ/n_π:

• The multiplicity dependence of the reconstruction efficiency is not equal for photons and pions. It is more sensitive to uncertainties of the detector parameters mentioned above for charged pions than for photon conversions. The reason of this is the large difference of Cherenkov photons produced in RICH-1 by a pion (usually with small β) compared to the collinear e^+e^- tracks from a conversion. The error introduced is ${}^{+6}_{-4} \cdot 10^{-4}$.

• Pions are reconstructed in a $p_\perp$-region from 1.3 to 2.5 GeV/c, which corresponds only to a small fraction of the pion production cross section. The measured yield is extremely sensitive to any change of the $p_\perp$-distribution with centrality of the collision. There is some evidence in our data for a subtle change of the average $p_\perp$ with $dN_{ch}/d\eta$. The effect would partially be compensated since the photon yield, also measured in a limited $p_\perp$-interval, would vary too. It is impossible to completely disentangle the effect of a changed pion $p_\perp$-distribution from an imperfect correction of the non-linear multiplicity scale. In any case the error of α is below $\pm\, 5 \cdot 10^{-4}$.

Because the reaction volume changes only little once target and projectile fully overlap, which corresponds to $dN_{ch}/d\eta \approx 110$ in our acceptance, the yield of direct photons should scale quadratically with $dN_{ch}/d\eta$ over most of the detected range. Their contribution is therefore determined by the slope parameter α extracted from the data. Convoluting statistical and systematical errors of α we can establish a bound for any thermal source of photons independent of the absolute normalization of the photon yield. We find upper limits of 7% (at 90% CL) and 9.5% (at 90% CL) from the multiplicity dependence of r_γ and n_γ/n_π, respectively. Note that the two approaches reach a similar precision, though the origins of the errors are quite different.

6 Conclusions

The inclusive photon production has been measured in S-Au collision at 200 GeV/u. In the kinematic region $2.1 < y < 2.65$ and 0.4 GeV/c $< p_\perp <$ 2.0 GeV/c the production rate as well as the shape of the photon $p_\perp$-spectrum are well described by known hadronic sources. A quantitative comparison limits any contribution of direct photons to the inclusive photon yield to less than 10% at a 90% confidence level. In addition the photon yield is proportional to $dN_{ch}/d\eta$ in the range from 75 up to 200, again the accuracy being limited by systematic errors. The uncertainty in the multiplicity dependence of r_γ sets a independent limit of 7% (at 90% CL) for the strength of a photon source with quadratic multiplicity dependence.

Our results are in good agreement with previous experiments which investigated O-Au [4] and, with lower statistics, O-W and S-W [3] at CERN SPS energies. Those experiments reached the conclusion that no unconventional source could be identified within $\approx 13 - 15\%$ systematical errors. The upper limit is now reduced by our data to 7%. Preliminary data of the WA80 group [15] showed an almost 15% contribution beyond photons from hadron decays with a significance at the 2–3 σ level. A recent – not yet completed – reanalysis of the data, points towards a smaller photon excess [21], bringing their result in better agreement with our findings.

The experimental accuracy reached today is still not good enough to draw a definite conclusion, since the predicted yield [1, 2] is at most comparable to the experimental errors. The search for direct photon emission remains an important issue, especially in the light of the enhanced dilepton production observed in S-induced reactions by our experiment [22], HELIOS-3 [23] and NA38 [24] (for a review see ref. [25]). For the continuation of the CERES experiment with lead beam [26] major improvements are being made to increase the sensitivity, i.e. to reduce the systematic errors. In particular, the measurement of the multiplicity dependence will benefit greatly from two new silicon drift detectors just behind the target which ease the identification of conversions and allow to determine event by event the exact charged multiplicity in the RICH acceptance.

The CERES collaboration acknowledges the good performance of the CERN PS and SPS accelerators. We are grateful for support by the German Bundesministerium für Forschung und Technologie under grant BMFT 06HD525I, the U.S. Department of Energy under Contract No. DE-AC02-76CH00016, the MINERVA Foundation, Munich/Germany, the H. Gutwirth Fund and the Israeli Science Foundation.

References

[1] M. Neubert, Z. Phys. C 42 (1989) 231;
J. Kapusta et al., Phys. Rev. D 44 (1991) 2774;
P.V. Ruuskanen, Nucl. Phys. A544 (1992) 169c;
R. Baier et al., Z. Phys. C 53 (1992) 433;
J. Kapusta, Nucl. Phys. A566 (1994) 45c
[2] E.V. Shuryak and L. Xiong Phys. Lett. B333 (1994) 316
[3] T. Åkesson et al., Z. Phys. C 46 (1990) 369
[4] R. Albrecht et al., Z. Phys. C 51 (1991) 1
[5] CERES/NA45-Collaboration, Proposal to the CERN SPSC 88-25, SPSC/P237
[6] R. Baur et al., Nucl. Instr. and Meth. A343 (1994) 87
[7] R. Baur et al., Nucl. Instr. and Meth. A343 (1994) 231;
R. Baur et al., Nucl. Instr. and Meth. A355 (1995) 329
[8] T. F. Günzel et al., Nucl. Inst. Meth. A316 (1992) 259
[9] W. Chen et al., IEEE Trans. Nucl. Sci. 39 (1992) 619
[10] CERN Program Library W5013
[11] T. Åkesson et al., Nucl. Phys. B353 (1991) 1
[12] R. Albrecht et al., Z. Phys. C 55 (1992) 539
[13] T. Åkesson et al., Z. Phys. C 46 (1990) 361
[14] D. Röhrich et al., Nucl. Phys. A566 (1994) 35c
[15] R. Santo et al., Nucl. Phys. A566 (1994) 61c
[16] A. Drees et al., Nucl. Phys. A566 (1994) 87c;
A. Schön, Doctoral thesis, Universität Heidelberg 1993, unpublished
[17] M. Aguilar-Benitez et al., Z. Phys. C 50 (1991) 405
[18] Review of Particle Properties, Phys. Rev. D 45 (1992) Part 2
[19] M. Bourquin, J.M. Gaillard, Nucl. Phys. B114 (1976) 334
[20] F. Büsser et al., Phys. Lett. B 55 (1975) 232;
J. Donaldson et al., Phys. Rev.Lett. 40 (1978) 684;
C. Kourkoumelis et al., Phys. Lett. B 84 (1979) 277;
J. Povlis et al., Phys. Rev.Lett. 51 (1983) 967;
M. Banner et al., Z. Phys. C 27 (1985) 329;
J. Antille et al., Phys. Lett. B 194 (1987) 568;
M. Bonesini et al., Z. Phys. C 42 (1989) 527
[21] T.C. Awes et al., Proceedings of QUARK MATTER 95, Monterey, California, USA
[22] G. Agakichiev et al., CERN-PPE/95-26, submitted to Phys. Rev. Lett.;
J.P. Wurm et al., Proceedings of QUARK MATTER 95, Monterey, California, USA
[23] M. Masera et al., Proceedings of QUARK MATTER 95, Monterey, California, USA
[24] M. C. Abreu et al., Nucl. Phys. A566 (1994) 77c
[25] I. Tserruya, Proceedings of QUARK MATTER 95, Monterey, California, USA
[26] CERES/NA45-Collaboration, Proposal to the CERN SPSC 94-01 , SPSC/P280

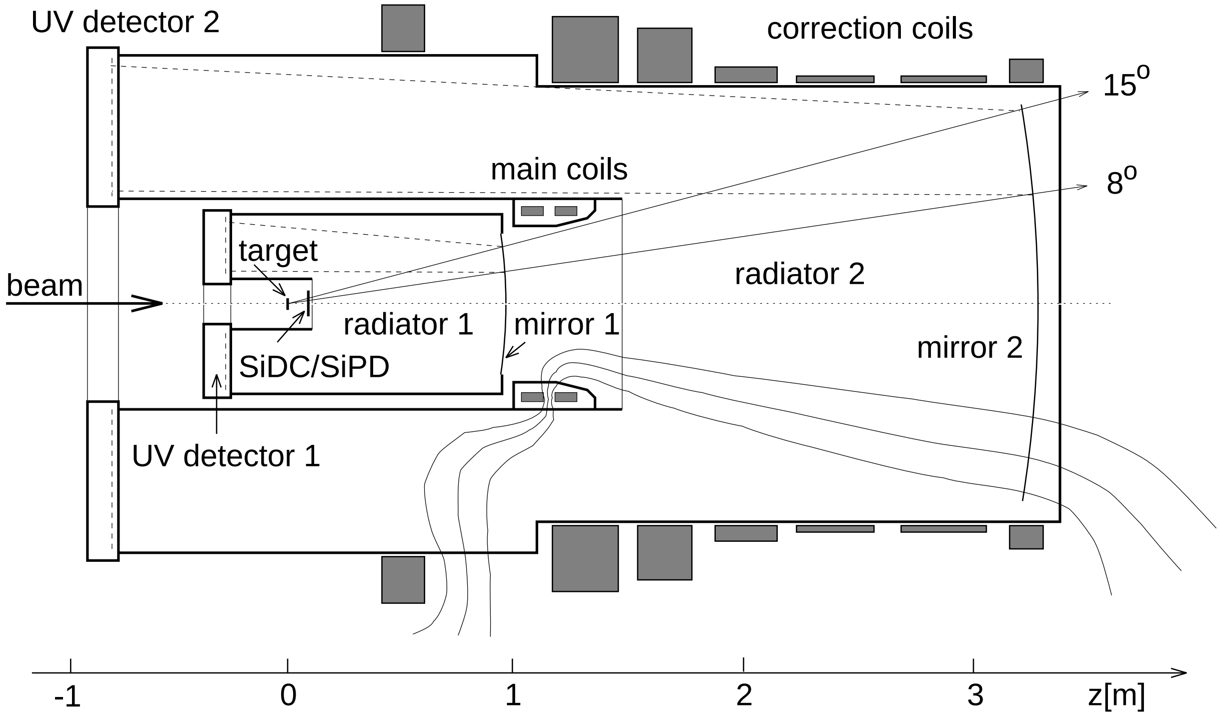

Figure 1: Schematic view of the CERES spectrometer

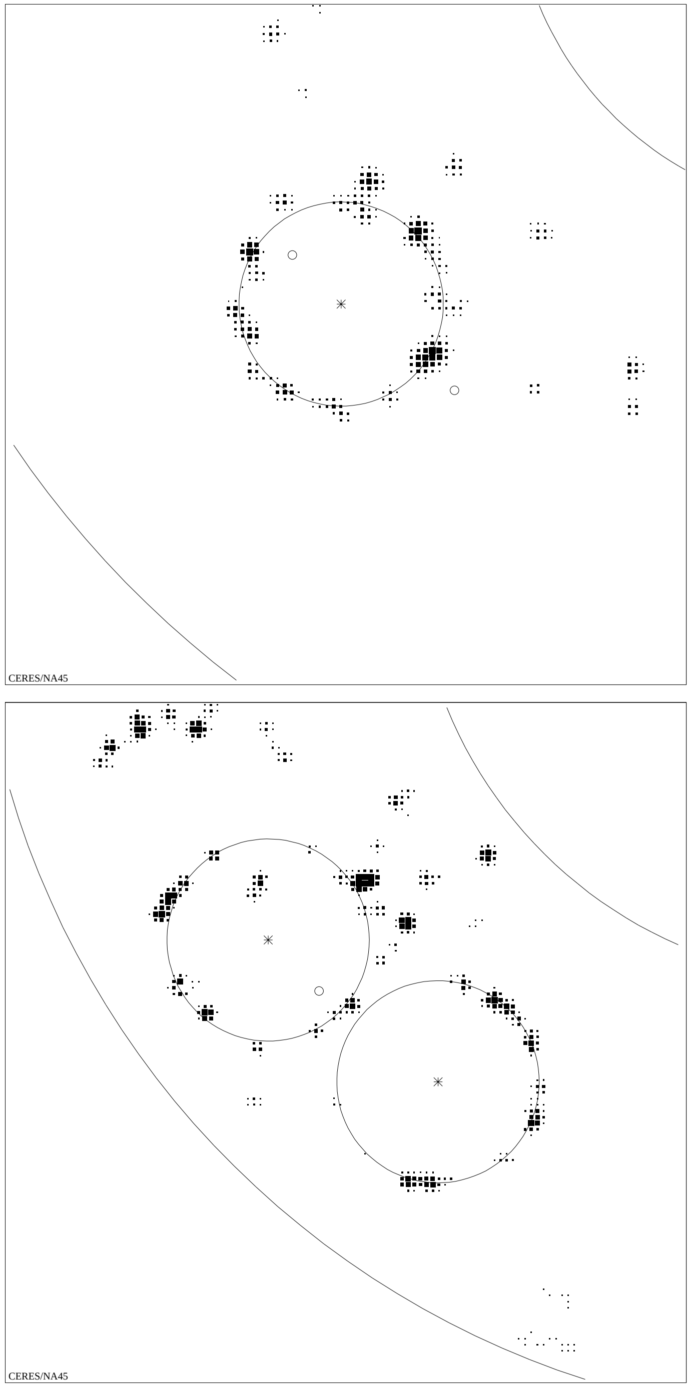

Figure 2: RICH display of a reconstructed photon conversion in a central S-Au collision. Clearly visible the typical V-pattern of a conversion: an unresolved double ring in RICH-1 (top) and two rings in RICH-2 (bottom). The area of the black boxes corresponds to the signal amplitude measured for each readout channel. The ring fits are shown with the ring centers (stars). The small circles mark the θ and φ-position of the rings in the other RICH.

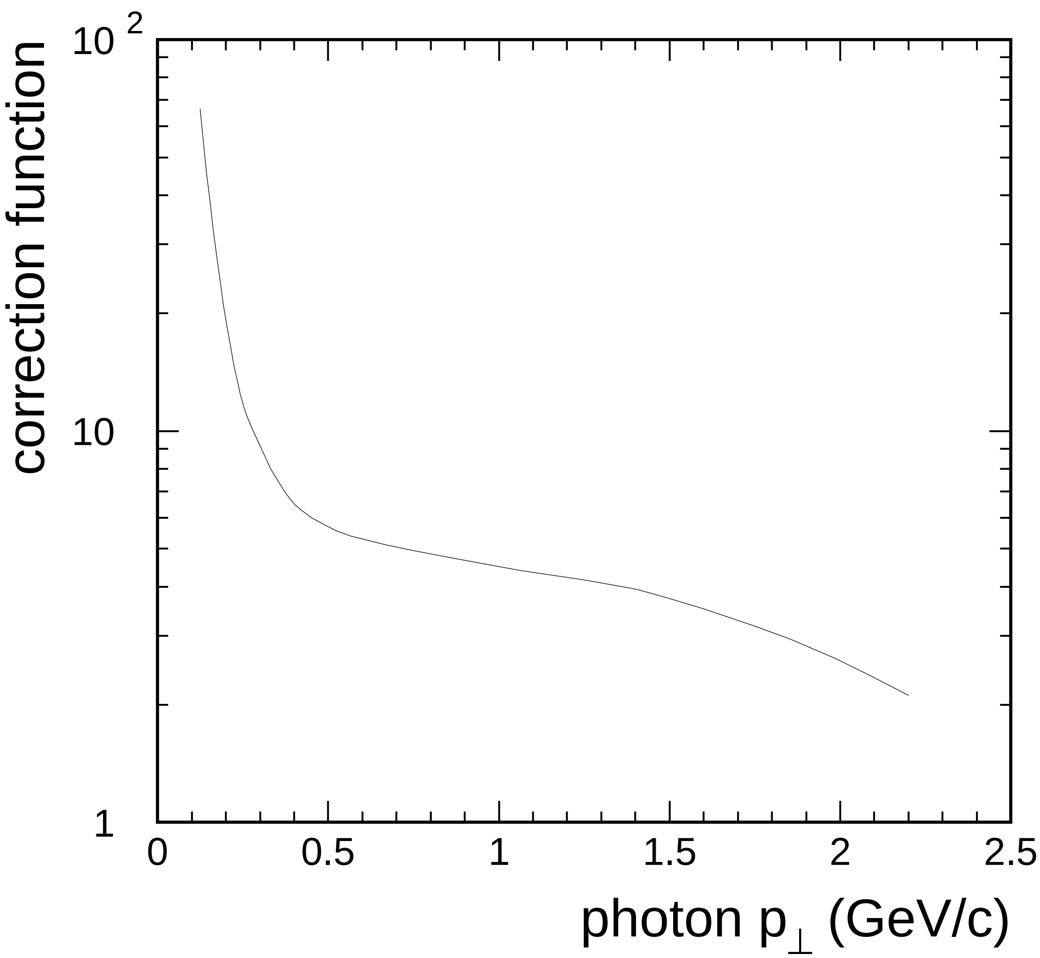

Figure 3: Function used to correct the photon $p_\perp$-spectrum for reconstruction efficiency. The Monte-Carlo simulation includes the acceptance of the spectrometer, losses caused by analysis cuts, and smearing due to momentum resolution.

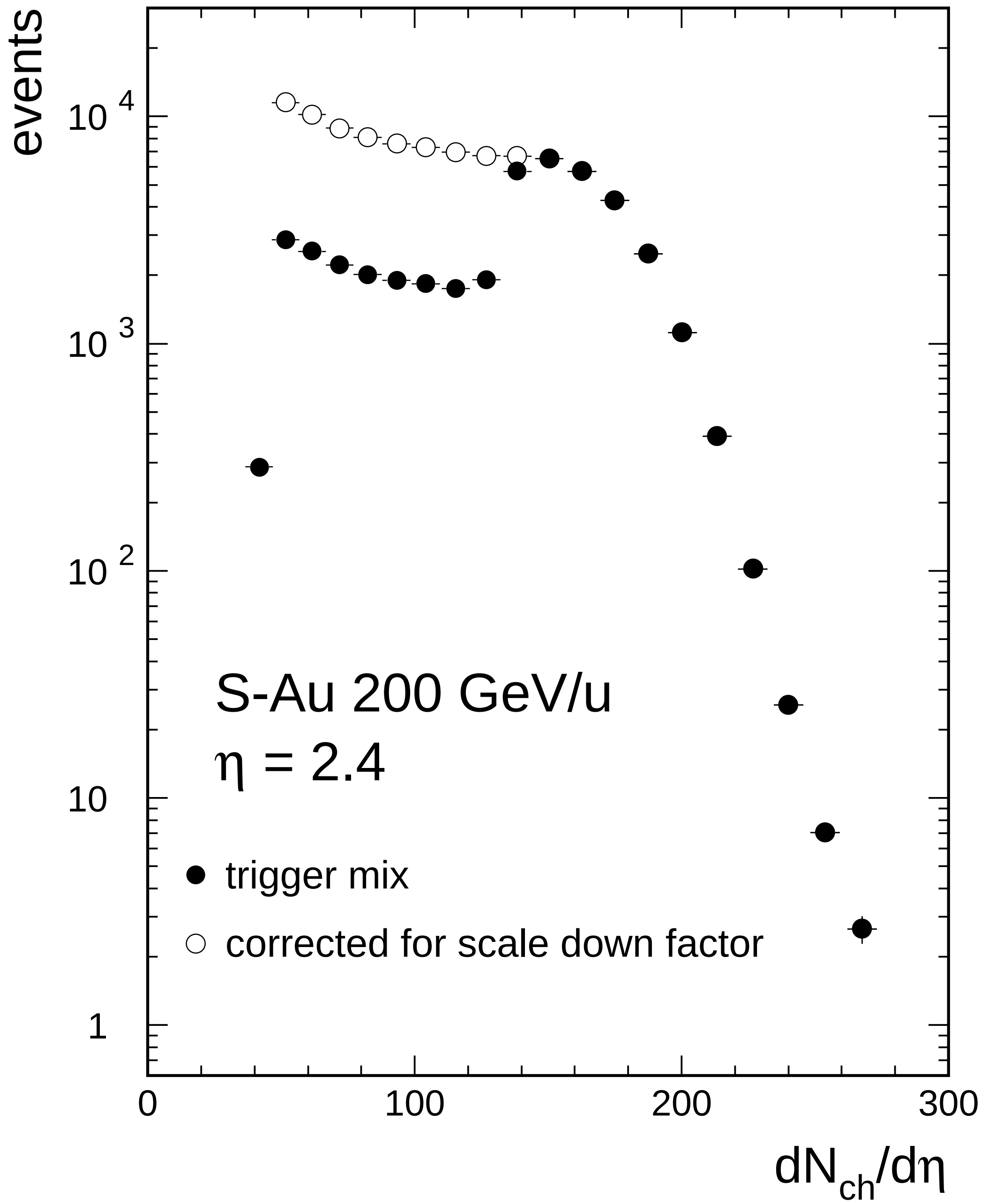

Figure 4: Multiplicity distribution for the S-Au data sample taken 1992 with two different multiplicity thresholds: a threshold at $dN_{ch}/d\eta = 140$ to select central collisions, and, in order to cover a large multiplicity range, a second threshold at $dN_{ch}/d\eta = 50$, which was scaled down by a factor of ~ 4. The open circles show the multiplicity distribution after rescaling the $dN_{ch}/d\eta > 50$ data.

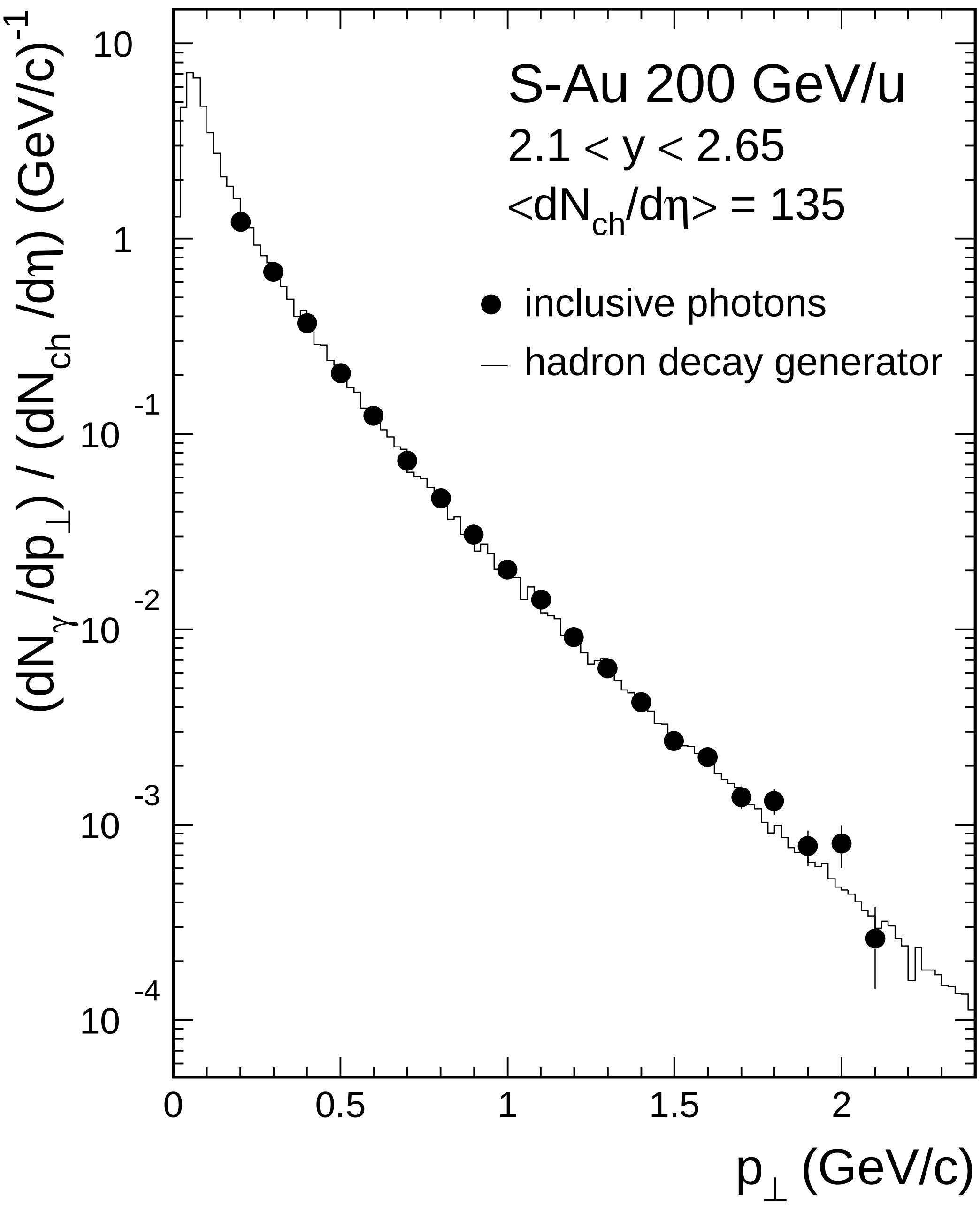

Figure 5: $p_\perp$-spectrum of photons from central S-Au collisions. Shown is the inclusive measurement (with statistical errors only) in comparison to the expectation from hadron decays, generated as described in the text.

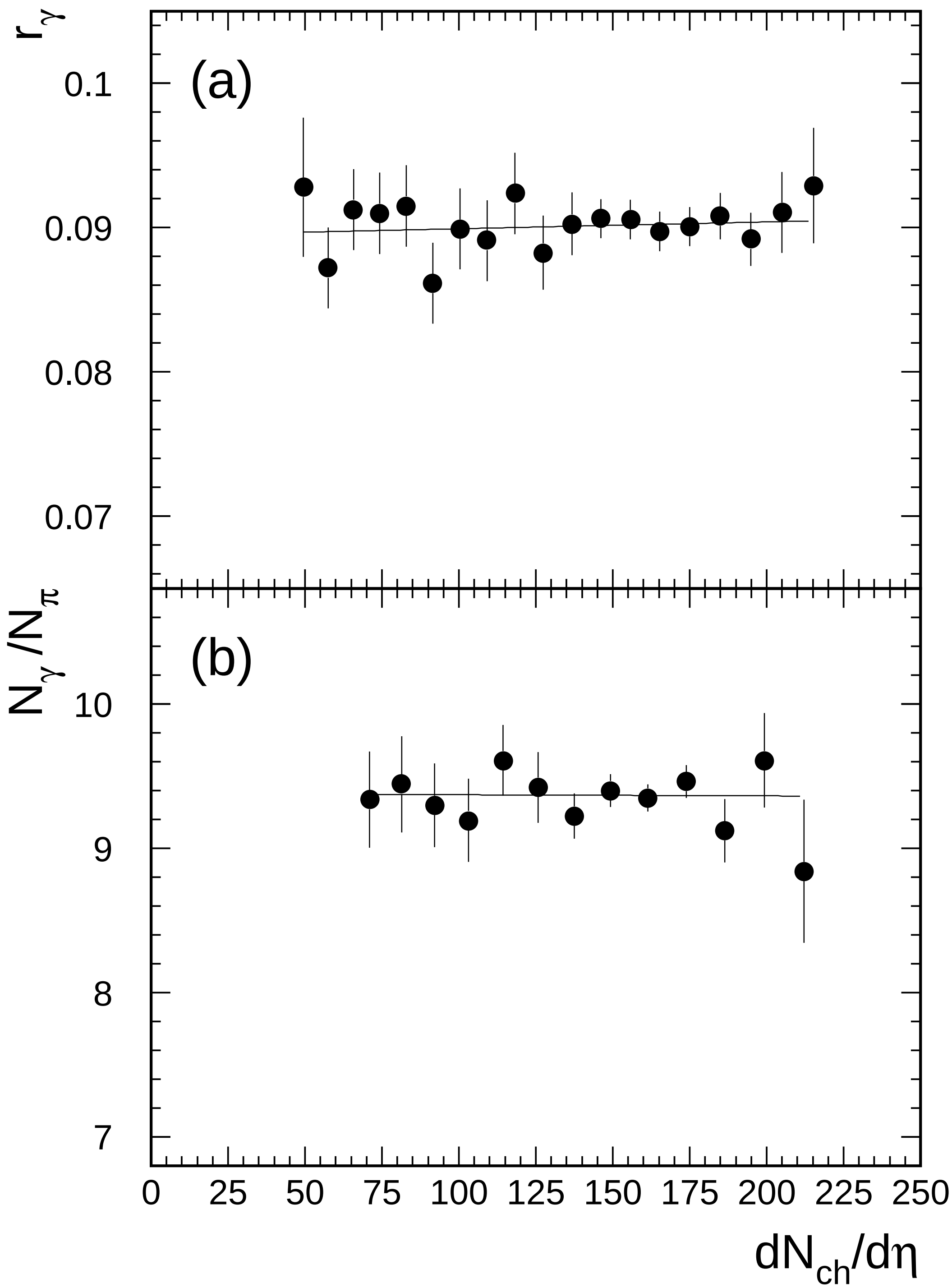

Figure 6: Multiplicity dependence of (a) r_γ as defined in Section 4, and (b) the ratio of measured inclusive photons ($0.4 < p_\perp < 2.0$ GeV/c) to charged pions ($1.3 < p_\perp < 2.5$ GeV/c). Only statistical errors are shown. In order to quantify a possible contribution of direct photons the data are fitted with $C(1 + \alpha \cdot dN_{ch}/d\eta)$.